Einstein-Podolsky-Rosen steering nonlocality in pulsed optomechanics and macroscopic atomic ensembles

Q. Y. He[1,2] and M. D. Reid[1]
[1] *Centre for Quantum Atom Optics, Swinburne University of Technology, Melbourne, Australia*
[2] *State Key Laboratory of Mesoscopic Physics, School of Physics, Peking University, Beijing 100871 China*

A specific scheme for creating Einstein-Podolsky-Rosen (EPR) entanglement between a mechanical oscillator and an optical pulse has been presented recently by Hofer et al [Phys. Rev. A **84**, 052327 (2011)]. Recent experiments have reported detection of EPR entanglement shared between spatially separated macroscopic atomic ensembles [Krauter et al, Phys. Rev. Lett. **107**, 080503 (2011) and Julsgaard et al, Nature **413**, 400 (2001)]. We adapt the theories developed for these types of experiments, and show how to optimise parameter regimes and measurement strategies, so that the EPR steering nonlocality (EPR paradox) can also be realised. For the first type of experiment, we show that asymmetric criteria will greatly improve prospects for detecting both entanglement and steering. For the second type, steering is predicted to be within experimental reach, but modification of the measurement scheme is required to ensure the possibility of spacelike separated measurement events.

I. INTRODUCTION

The Einstein-Podolsky-Rosen (EPR) paradox [1] has been quite extensively explored for optical fields, both for continuous variable (CV) [2–7] and discrete [8, 9] measurement outcomes. The evidence for the EPR nonlocality is convincing, with some experiments obtaining EPR correlations for high detection efficiencies, though not yet also for spacelike separated measurement events. The EPR paradox has been confirmed for single photon pairs [10], and mesoscopically, for the quadrature phase amplitudes [2] and Stokes polarisation observables of twin optical beams [11] and optical pulses [12].

The EPR paradox reveals incompatibility between the assumption of local realism, and the completeness of quantum mechanics. As an example, consistency would demand that the physical quantities associated with noncommuting observables are predetermined, prior to measurements, more than can be explained by the Heisenberg uncertainty principle. Recently, work by Wiseman, Jones and Doherty [13, 14] has revealed that the EPR paradox is a realisation of quantum steering, a form of nonlocality identified by Schrodinger [15] where measurements made by one observer at a location A can apparently "steer" the state of another observer, at location B. Following [16] and [17], we therefore use the term "EPR steering" (or "steering" for simplicity) throughout this paper to refer to this particular kind of nonlocality, i.e. the EPR paradox.

EPR steering can thus be viewed as a strong form of entanglement, for which a certain type of nonlocality manifests. Steering is generally easier to verify than Bell's form of nonlocality that falsifies local realism, though, in terms of understanding what theories will correctly describe nature, may be less informative. Despite that, the EPR paradox and steering have been shown to have a special usefulness to quantum information tasks [18–21], including one-sided device independent cryptography [22] and secure teleportation [23]. For these reasons, both fundamental and applied, and perhaps because of steadily improving technology, there has been an escalation in the amount of theoretical interest [16, 24–29] and in the number of experiments reporting an EPR steering nonlocality [5, 17, 30–32]. In fact, recent experiments realise EPR steering for photonic qubits, without detection efficiency loopholes [33, 34], and for spacelike separated measurement events [35].

The evidence however for steering with massive particles is almost nonexistent. The Bell nonlocality correlation strength has been verified without detection efficiency loopholes for ions [36] and for qubits in solid state systems [37], but not for significant spatial separations.

We are therefore motivated to analyse the possibility of realising steering for systems of massive particles. There have already been a number of proposals to detect EPR or Bell nonlocality utilising cold atoms or Bose-Einstein condensates (BEC) [38]. These include proposals to detect CV EPR steering using four wave mixing [39], or using static and dynamical processes involving atoms confined to an optical lattice [40–42]. Twin atom beams [43, 44] with EPR-type correlated quadratures have been created in a recent experiment [45], in a process of pair creation that is similar to that used in optics, although EPR steering has not been reported.

In this paper we examine two alternative physical systems not yet studied for EPR steering, but that enable realisation of quantum limited noise levels. These are optomechanical oscillators and macroscopic room temperature atomic ensembles. We analyse the theory of two specific experiments, that either demonstrate, or have the potential to demonstrate, an EPR-type entanglement (EPR-type entanglement is that entanglement existing between two spatially separated systems, so that EPR-type correlations can be realized), and propose how the steering nonlocality might be generated and verified, in each case. Both theories model realistically the decoherence that arises due to thermal reservoirs, and we show in both cases that steering is predicted possible over the

parameter range considered feasible for the generation of entanglement.

First, in Section III, we study the recently proposed scheme of Hofer et al [46], to generate EPR-type entanglement between the quadratures of a mechanical oscillator and an optical pulse, using the radiation pressure interaction between the optical cavity mode and the cavity mirror. A similar proposal was put forward originally by Giovannetti et al [47]. We adopt the theoretical model developed by Hofer et al, and give predictions for steering over the parameter range examined by them. Clearly, the realisation of steering is a greater challenge than obtaining an entanglement. However, for this system in which thermal noise plays an asymmetric role, we show that the use of asymmetric entanglement and steering criteria [3, 48] will greatly increase the possibility of observing both entanglement and steering. One-way steering [24, 31] is predicted for all values of squeeze parameter, while two-way steering becomes possible above a threshold value.

Second, in Section IV, we examine the experiments of Julsgaard et al [49], Krauter et al [50], and Muschik et al [51] involving two room temperature macroscopic atomic ensembles, for which an EPR-type entanglement has already been measured. In this case, modification of the experiment is necessary to ensure at least the possibility of two spacelike separated measurement events. The reported correlation between the macroscopic atomic ensembles is not sufficient to demonstrate steering, but our analysis of the theory developed by Muschik et al [51, 52] reveals how to optimise for this form of nonlocality. EPR steering is predicted possible within the limits of the parameters reported for the experiments, provided one can employ local detection of the EPR observables, so that conditional measurements can be realised.

II. THE EPR STEERING NONLOCALITY: DEFINITIONS AND CRITERIA

A. Definition and the LHS model

The work of Wiseman et al [13] showed that there are three distinct types of quantum nonlocality, depending on the restriction placed on the local hidden variable (LHV) theory involved to model the measured statistics. We consider bipartite nonlocality, where local measurements are made on two spatially separated subsystems, identified as A and B. The observers making measurements at these two locations are often called Alice and Bob respectively. The LHV model introduced by Bell [53] identifies two local "hidden" states, one for each site. In this model, the predictions for moments of the joint measurements made at the two spatially separated sites are given by

$$\langle X_A X_B\rangle = \int_\lambda d\lambda P(\lambda)\langle X_A\rangle_\lambda\langle X_B\rangle_\lambda. \qquad (1)$$

Here X_j are the possible results for a measurement $\hat{X}_j$ at site j where $j = A, B$, $\langle X_j\rangle_\lambda$ is the expected value of X_j for a given set $\{\lambda\}$, and $P(\lambda)$ is the hidden variable probability distribution function. Nonlocality occurs when this LHV model is falsified. Bell nonlocality is the case when there is no other constraint placed on the local hidden states. Bell's nonlocality reveals a failure of all LHV theories (1) to describe the measured statistics.

Subsets of LHV theories can be created in which one, or all, of the local hidden states associated with a set of spatial locations are constrained to be consistent with the predictions of a quantum state. In this case, the model (1) is called a local hidden state (LHS) model [13, 14, 16]. We demonstrate a steering and entanglement nonlocality when a failure of the LHV is established, where the restriction applies to one, or all, sites respectively [13, 25]. The definitions are qualified by noting that in all cases, the nonlocality is to be demonstrated by way of spacelike separated local measurements at each of the sites.

In the bipartite case, the LHV model (1) applies. The model is a quantum separable model, if both local hidden states are constrained to predict quantum statistics, meaning that the local averages $\langle X_j\rangle_\lambda$ $(j = A, B)$ are each consistent with a quantum state prediction i.e. can be generated by a local quantum density operator. Entanglement as a nonlocality is verified when the quantum separable model is falsified. Steering occurs in the asymmetric case, where the LHS model that is falsified assumes only one local hidden state to be constrained to predict quantum statistics. It was shown in Refs. [13, 14] that the quantum states demonstrating Bell nonlocality are a strict subset of the states demonstrating steering, which are again a strict subset of all entangled states.

B. Continuous variable EPR steering criteria

We focus in this paper on CV measurements, where the outcomes of measurements are continuous variables. We consider two conjugate observables, X_j and P_j at each site $j = A, B$, scaled such that $\Delta X_j \Delta P_j \geq 1/4$ (we are using normalised quadratures with $\left|\langle[X_B, P_B]\rangle\right| = 1/2$). The observables might correspond to a scaled position and momentum, or field mode quadrature phase amplitudes. It has been shown that the Einstein-Podolsky-Rosen paradox [48] and steering ("EPR steering") of B by A [13, 16, 48] is realised if

$$\Delta_{inf,A} X_B \Delta_{inf,A} P_B < 1/4, \qquad (2)$$

where $\Delta^2_{inf,A} X_B \equiv \Delta^2(X_B|O_A)$ and $\Delta^2_{inf,A} P_B \equiv \Delta^2(P_B|O'_A)$ are the variances of the conditional distributions $P(X_B|O_A)$ and $P(P_B|O'_A)$. Here O_A, O'_A are arbitrary observables for system A, usually selected to minimise the variance product [3, 16, 54]. For the EPR experiments, the choice is usually either $O_A \equiv X_A$ and $O'_A \equiv P_A$, or the reverse choice, depending on the correlation of the systems. It has been shown that the criterion (2) is necessary and sufficient for steering in the

case of the so-called Gaussian states and Gaussian CV (quadrature phase amplitude) measurements [13] (provided the observables for Alice are suitably selected). In this paper, we examine the predictions for the CV steering criterion (2), although the LHS model has been used to derive other steering nonlocality criteria, including for qubits [16], qudits [29] multi-observable [17, 34] and multipartite scenarios [25, 29].

We note that since $x^2+y^2 \geq 2xy$ for any real numbers, the steering criterion (2) also implies the following sum criterion for steering [3]. EPR steering of B by A is confirmed if

$$\Delta^2_{inf,A} X_B + \Delta^2_{inf,A} P_B < 1/2 \quad (3)$$

since, using the identity, (3) implies (2). This sum criterion, which can also be derived directly from the LHS model of [13] (see Appendix I), will be useful to us in Section III, to give predictions for steering in the presence of mechanical decoherence.

We note the inherent asymmetry of the steering criterion Eq. (2). The asymmetry reflects the asymmetric nature of the original EPR paradox, in which it is the reduced noise levels of Alice's predictions for Bob's system that are relevant in establishing the paradox [1]. We will show that the use of an asymmetric criterion becomes a particularly important consideration, even for detecting entanglement, where decoherence affects the two systems asymmetrically [24, 31].

C. Symmetric entanglement and steering criteria

EPR-type entanglement between two modes represented by A and B can be verified experimentally using the criterion proposed by Duan et al [55]. For the original EPR gedanken experiment [1], a correlation exists between X_A and X_B, and an anticorrelation exists between P_A and P_B. In this case, the entanglement is verified if the sum and difference variances are reduced, according to

$$\Delta_{ent} = \Delta^2(X_A + X_B) + \Delta^2(P_A - P_B) < 1. \quad (4)$$

The exact choice of observables for the A field depends on the details of the correlation of the EPR system. For example, the observation of

$$\Delta_{ent} = \Delta^2(X_A + P_B) + \Delta^2(P_A + X_B) < 1 \quad (5)$$

is also sufficient to confirm entanglement between the two spatially separated systems. We use the notation Δ_{ent} in either case, to imply an observation of entanglement via a measurement of a reduced noise level. It has been noted [3, 39] that the measurement of

$$\Delta_{ent} < 1/2 \quad (6)$$

is also sufficient to indicate steering. In fact, because of the symmetry in relation to the systems A and B for the criteria (4) and (5), the observation of $\Delta_{ent} < 1/2$ will indicate two-way steering (that A steers B, and also that B steers A) [31].

D. Asymmetric entanglement criteria

Where there is asymmetry in the system, the symmetric criteria (4-5) become less sensitive to entanglement. Other witnesses of entanglement, including necessary and sufficient measures, have been analysed for Gaussian states [56, 57], but we will focus here on the local uncertainty relations (LUR) entanglement criteria, for which entanglement manifests as a reduction in variance caused by an EPR-type correlation. As outlined in the Appendix A, entanglement between modes A and B is confirmed when

$$\Delta^2(X_B - g_x X_A) + \Delta^2(P_B + g_p P_A) < \frac{1 + g_x g_p}{2}, \quad (7)$$

or when

$$\Delta^2(X_B + g'_x P_A) + \Delta^2(P_B + g'_p X_A) < \frac{1 + g'_x g'_p}{2}, \quad (8)$$

where g_x, g'_x, g_p, g'_p are arbitrary real constants that can be chosen to optimise the entanglement measure, i.e. to minimise the variance sum combination.

Other useful entanglement criteria follow by considering variance products [57, 58] (see Appendix A). Entanglement is verified if

$$\Delta^2(X_B + g_x P_A)\Delta^2(P_B + g_p X_A) < \left(\frac{|g_x g_p| + 1}{4}\right)^2. \quad (9)$$

This criterion is useful, since if (9) holds, the sum criterion (8) will also hold and (9) is equivalent to

$$\Delta^2(X_A + h_x P_B)\Delta^2(P_A + h_p X_B) < \left(\frac{|h_x h_p| + 1}{4}\right)^2, \quad (10)$$

where $h_x = 1/g_x$ and $h_p = 1/g_p$, which implies a symmetry of entanglement detection between the two systems.

III. EPR STEERING IN PULSED OPTOMECHANICS

There have been proposals to realise EPR correlations between a mechanical oscillator and an optical mode [47]. In these proposals, an EPR correlation is generated between the position and momentum quadratures X_B and P_B of the oscillator, and the quadrature phase amplitudes X_A, P_A defined for the optical field. Recent proposals suggest to employ pulsed optomechanics to prepare and verify quantum states [59], and a specific scheme for entangling a mechanical oscillator and an optical pulse that incorporates sources of decoherence has been presented by Hofer et al (HWAH) [46]. We examine this scheme, in order to understand how it may be modified to detect steering.

A blue detuned light pulse is input to an optomechanical cavity mode and interacts with the oscillator mirror mode via radiation pressure [60], as described by Hofer

et al, and depicted in the Fig. 1. The boson creation and destruction operators for the optical and mechanical modes are a_c, $a_c^\dagger$ and a_m, $a_m^\dagger$ respectively. Quadrature phase amplitudes $X_{c/m}$, $P_{c/m}$ are defined according to $a_c = k(X_c + iP_c)$ and $a_m = k(X_m + iP_m)$, where k is chosen to ensure the normalised EPR inequality (2). The key physical parameters are the interaction strength g, the oscillation frequency ω_m and dissipation rate γ, the optical cavity resonance frequency ω_c and decay rate κ, the pulse carrier frequency ω_1 and duration time τ, and n_0 the initial occupation of the thermal state of the mirror.

A. Generation of EPR-type entanglement

The effective Hamiltonian [58, 60] for the system in a frame rotating at the laser frequency is

$$H = \omega_m a_m^\dagger a_m + \Delta_c a_c^\dagger a_c + g(a_m + a_m^\dagger)(a_c + a_c^\dagger), \quad (11)$$

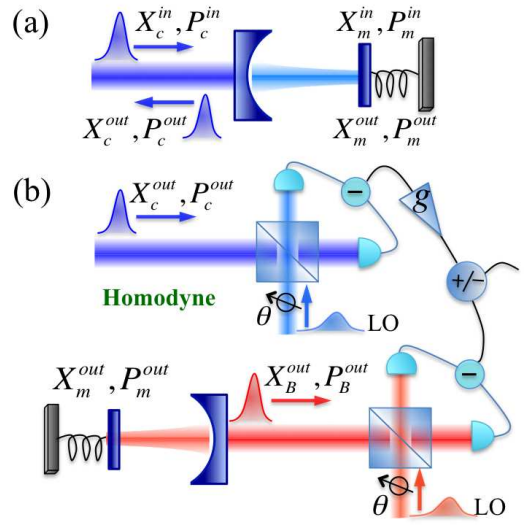

Figure 1: (Color online) Measurement of the EPR entanglement and steering between an oscillator and a pulse. *Step I: Entangling a pulse with a mechanical oscillator.* (a) Following HWAH, the blue-detuned pulse interacts with an optomechanical system. The output pulse quadrature phase amplitudes X_c^{out}, P_c^{out} are EPR correlated with the final quadratures X_m^{out}, P_m^{out} of the mechanical oscillator, according to $X_c^{out} \sim -P_m^{out}$ and $P_c^{out} \sim -X_m^{out}$, in the limit of a large squeezing parameter r. *Step II: To verify the steering.* (b) The output pulse amplitudes X_c^{out}, P_c^{out} are measured by homodyne detection. The quadratures of the oscillator are measured by interacting the cavity with a second red-detuned pulse. The outputs X_B^{out}, P_B^{out} are a direct measure of the original oscillator quadratures, X_m^{out}, P_m^{out}, according to $X_B^{out} = -P_m^{out}$ and $P_B^{out} = X_m^{out}$, in the appropriate limit which optimises the measurement process. To measure steering, and to optimise measurement of entanglement, the difference currents are combined asymmetrically, by introducing an adjustable relative gain factor g.

where $\Delta_c = \omega_c - \omega_1$ is the detuning of the cavity with respect to the laser [46]. The term in g describes the linearised optomechanical coupling due to the radiation pressure, and comprises a beam splitter-type coupling interaction and a two-mode squeezing type interaction [61, 62], that is known to generate entanglement [48].

We now summarise the approach of HWAH. The pulse shape is assumed to be flat-top and to possess a smooth head and tail. HWAH propose the pulse to be either blue-detuned, or red-detuned to the cavity resonance [46], to enable the choice to enhance either the two-mode squeezing interaction term, for the creation of entanglement, or the beam splitter-type interaction term, for the purpose of measurement.

Entanglement is created using a blue detuned pulse. In the case where $g \ll \kappa \ll \omega_m$, and after neglecting mechanical decoherence effects, HWAH derive a set of idealised Langevin equations for the mode operators. To justify neglecting mechanical decoherence, they assume the pulse duration and time taken for the entire protocol to be very short compared to the mechanical decoherence time. For the blue detuned pulse, after using the parameter restrictions to justify a rotating wave approximation (RWA) and an adiabatic solution for the cavity mode, the simplified Langevin equations lead to solutions for quadratures X_c^{out}, P_c^{out} of the output pulse, in terms of the input pulse quadratures X_c^{in}, P_c^{in} and the initial (input) quadratures X_m^{in}, P_m^{in} of the mechanical mode. The solutions are

$$\begin{aligned} X_c^{out} &= -e^r X_c^{in} - \sqrt{e^{2r}-1}P_m^{in}, \\ P_c^{out} &= -e^r P_c^{in} - \sqrt{e^{2r}-1}X_m^{in}, \\ X_m^{out} &= e^r X_m^{in} + \sqrt{e^{2r}-1}P_c^{in}, \\ P_m^{out} &= e^r P_m^{in} + \sqrt{e^{2r}-1}X_c^{in}, \end{aligned} \quad (12)$$

where X_m^{out} and P_m^{out} are the final quadratures of the mechanical oscillator, and $r = g^2\tau/\kappa$ is the squeezing parameter that is dependent on the strength of the interaction and the duration of the pulse. The solutions in the limit of large r become $X_c^{out} = -e^r(X_c^{in} + P_m^{in})$, $P_c^{out} = -e^r(P_c^{in} + X_m^{in})$, $X_m^{out} = -P_c^{out}$ and $P_m^{out} = -X_c^{out}$. We use the subscript c for the pulse quadratures, for convenience, and stress the distinction between these input/ output pulse quadratures and the internal cavity mode quadratures [46, 63].

The input/ output solutions allow ready calculation of the entanglement and steering criteria of Sec. II. The result for the entanglement criterion (5) is [46]

$$\begin{aligned} \Delta_{ent} &\equiv \Delta^2(X_m^{out} + P_c^{out}) + \Delta^2(P_m^{out} + X_c^{out}) \\ &= (n_0+1)(e^r - \sqrt{e^{2r}-1})^2, \end{aligned} \quad (13)$$

where n_0 is the initial occupation of the oscillator. Our choice of scaling means that entanglement is obtained when $\Delta_{ent} < 1$. Further, because we wish to distinguish entanglement from the steering, we use the subscript "ent" to denote entanglement. In fact, $\Delta_{ent} = \frac{1}{2}\Delta_{EPR}$

where Δ_{EPR} is the entanglement measure specified in the Ref. [46]. For this system, the EPR correlation is between X_m^{out} and P_A^{out}, and P_m^{out} and X_A^{out}.

The solutions (13) reveal that for large r, $\Delta_{ent} \rightarrow (n_0+1)e^{-2r} \rightarrow 0$. This suggests that, potentially, an arbitrary amount of EPR correlation, and hence steering, can be obtained. The effect of the initial occupation number n_0 will be an important factor in determining the feasibility of the experiment, however, since there is always a practical limitation on the value of r that can be achieved experimentally. Figure 2 plots the minimum value r_0 of r required for a given excitation n_0, revealing the logarithmic dependence

$$r > r_0 = ln\frac{n_0+2}{2\sqrt{n_0+1}} \overset{n_0\rightarrow\infty}{\sim} \frac{1}{2}\ln n_0 \tag{14}$$

discussed in Ref. [46]. We next study the predictions for the asymmetric entanglement measures (8-10), to show an optimisation is possible, so that entanglement can be detected for lower values of r, for any given n_0.

B. Detecting entanglement

There is asymmetry in the optomechanical system, since the occupation number n_0 cannot be assumed negligible for the mechanical oscillator as is justified for the optical mode. For this reason, the asymmetric optimized criteria (8-10) become extremely useful for detecting entanglement in the oscillator-pulse system.

Entanglement between modes A and B is confirmed by (8) when

$$\Delta_{g,ent} = \frac{\Delta^2(X_m^{out}+g_xP_c^{out})+\Delta^2(P_m^{out}+g_pX_c^{out})}{(1+g_xg_p)/2} < 1. \tag{15}$$

The $\Delta_{g,ent}$ can be minimized by the optimal factor g_x, g_p via the variational method [3, 42, 48], by setting $\partial D_{g,sum}/\partial g_{x,p} = 0$. For light initially in vacuum $\Delta^2 X_c^{in} = \Delta^2 P_c^{in} = 1/4$ and the mirror in a thermal state with $\Delta^2 X_m^{in} = \Delta^2 P_m^{in} = n_0/2 + 1/4$, we find the optimal choice is

$$g_x = g_p = \frac{n_0/(n_0+1)+\sqrt{[n_0/(n_0+1)]^2+4e^{2r}(e^{2r}-1)}}{2e^r\sqrt{e^{2r}-1}}. \tag{16}$$

Entanglement can be also confirmed by the product criterion (9)

$$\Delta_{g,prod} = \frac{\Delta^2(X_m^{out}+g_xP_c^{out})\Delta^2(P_m^{out}+g_pX_c^{out})}{[(|g_xg_p|+1)/4]^2} < 1, \tag{17}$$

which can also be minimized by selecting an optimal factor g_x, g_p. We find the optimal values of g_x and g_p are the same (Eq. (16)) as those given for the sum criterion.

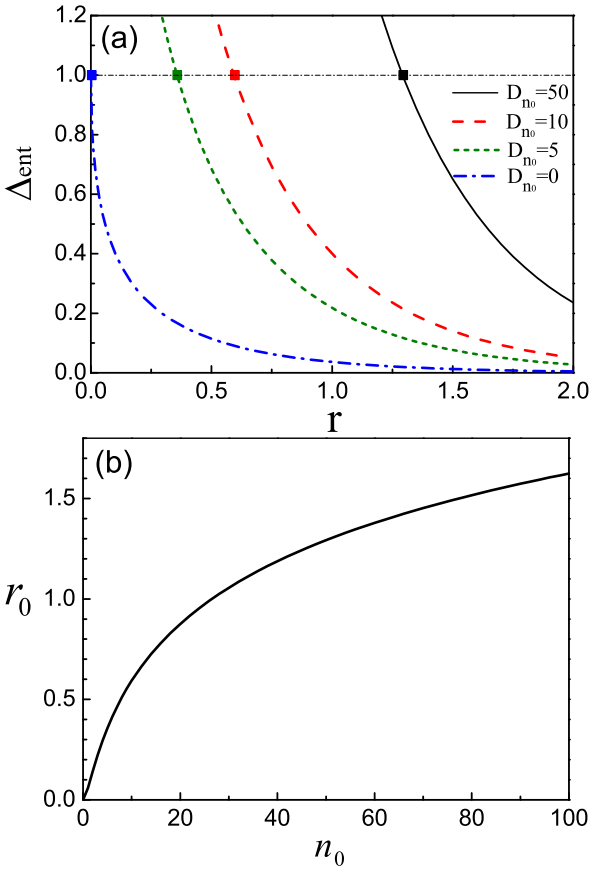

Figure 2: (Color online) Entanglement detected using the symmetric criterion Δ_{ent} of Eq. (13). Entanglement between the oscillator and the optical pulse is detected if $\Delta_{ent} < 1$. Here, $\Delta_{ent} = \frac{1}{2}\Delta_{EPR}$ where Δ_{EPR} is the entanglement measure specified by HWAH [46]. (a) Δ_{ent} is plotted versus the squeeze parameter r for various values $n_0 = 0,\ 5,\ 10,\ 50$, where n_0 is the initial mechanical oscillator occupation number. (b) The minimum strength r_0 of the squeezing parameter required, for a given n_0 in order to detect entanglement via the criterion $\Delta_{ent} < 1$.

The entanglement witnesses $\Delta_{g,ent}$, $\Delta_{g,prod}$ are plotted versus r, for various values of initial occupation number n_0 of the oscillator, in Fig. 3. We find the criteria are symmetric with respect to interchange of the two systems, provided the reciprocals of the values of g_x and g_p are taken, as explained in Section II. The asymmetric criteria with optimal gain factors, both in the sum and product forms, are more sensitive to entanglement than the symmetric entanglement witness Δ_{ent}, which is restricted to consider $g_x = g_p = 1$.

We note there is a substantial difference between the predictions in the symmetric and asymmetric case. Unlike the symmetric criterion (which showed a logarithmic dependence $r_0 = \frac{1}{2}\ln n_0$ of the minimum r_0 required for entanglement detection with n_0, for large n_0), the asymmetric criteria involving $\Delta_{g,ent}$ or $\Delta_{g,prod}$ are not sensitive to n_0, for large n_0. For a given n_0, we can always show entanglement for any $r > 0$, provided one can

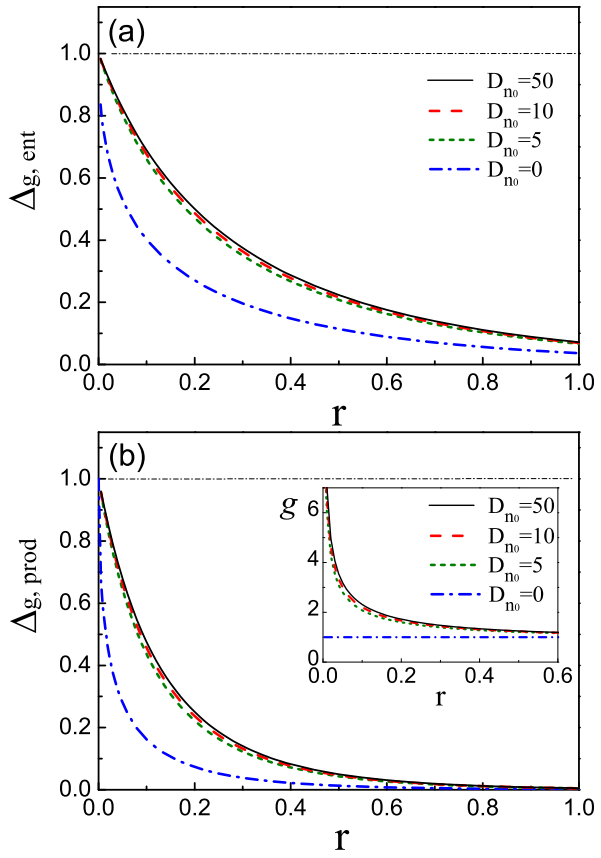

Figure 3: (Color online) Entanglement detected using the asymmetric criteria (7-10). (a) $\Delta_{g,ent}$ (Eq. (15)) (b) $\Delta_{g,prod}$ (Eq. (17)) are plotted versus the squeezing parameter r for values $n_0 = 0,\ 5,\ 10,\ 50$ giving the initial occupation number of the oscillator. Entanglement between an oscillator and a pulse is observed when $\Delta_{g,ent} < 1$ or $\Delta_{g,product} < 1$. The optimal $g_x(g_p)$ to minimize $\Delta_{g,ent}$ and $\Delta_{g,prod}$ is shown in the inset of (b). The results indicate improved detection of the entanglement, for large n_0.

select the optimal choice of gain factor g_x, g_p. The minimum value r_0 required for entanglement detection via the asymmetric criteria is not (directly) limited by n_0, but will depend in practice on the accuracy achieved for selecting the gain factors, which become large, for the smaller r values in the high n_0 limit.

C. Detecting steering

We next evaluate the steering predicted by the output solutions (12). The linear relations of the output with respect to the inputs ensure Gaussian conditional distributions [3], and the EPR variances are readily evaluated based on an accuracy of inference, that an observer at A measuring the output pulse quadratures can predict the result for the quadrature X_m^{out} of the oscillator, to a certain measurable level of uncertainty. A simple way to determine this uncertainty for Gaussian distributions is to use a linear estimate $g_x P_c^{out}$, based on the result P_c^{out} for measurement at A [3, 42, 48]. We find

$$\Delta^2_{inf}(X_m^{out}|P_c^{out}) \;=\; \Delta^2(X_m^{out} + g_x P_c^{out}), \qquad (18)$$

where $g_x = -(\langle X_m^{out}, P_c^{out}\rangle + \langle P_c^{out}, X_m^{out}\rangle)/2\Delta^2 P_c^{out}$ is optimised to minimise the variance $\Delta^2_{inf}(X_m^{out}|P_c^{out})$. Comparing to the definition of conditional variances $\Delta^2_{inf,A} X_B \equiv \Delta^2(X_B|O_A)$ introduced under Eq. (2), here we have selected P_c^{out} as observable O_A, to obtain the conditional variance $\Delta^2_{inf}(X_m^{out}|P_c^{out})$.

Similarly, the conditional variance $\Delta^2_{inf}(P_m^{out}|X_c^{out}\rangle$ is evaluated as

$$\Delta^2_{inf}(P_m^{out}|X_c^{out}) \;=\; \Delta^2(P_m^{out} + g_p X_c^{out}), \qquad (19)$$

where $g_p = -(\langle P_m^{out}, X_c^{out}\rangle + \langle X_c^{out}, P_m^{out}\rangle)/2\Delta^2 X_c^{out}$ is optimised to minimise the conditional variance.

The steering of the mechanical oscillator by the pulse can be confirmed when (we use the EPR criterion (2))

$$E_{steer}(M|C) = 4\Delta_{inf}(X_m^{out}|P_c^{out})\Delta_{inf}(P_m^{out}|X_c^{out}) < 1. \qquad (20)$$

For light initially in vacuum $\Delta^2 X_c^{in} = \Delta^2 P_c^{in} = 1/4$ and the mirror in a thermal state with $\Delta^2 X_m^{in} = \Delta^2 P_m^{in} = n_0/2 + 1/4$, we can calculate the prediction for steering. We find

$$\begin{aligned}\Delta^2_{inf}(X_m^{out}|P_c^{out}) \;&=\; \Delta^2(X_m^{out} + g_x P_c^{out}) \\ &=\; (e^r - g_x\sqrt{e^{2r}-1})^2\Delta^2 X_m^{in} \\ &\quad +(\sqrt{e^{2r}-1} - g_x e^r)^2\Delta^2 P_c^{in} \qquad (21)\end{aligned}$$

which can be minimized by optimizing the factor g_x via $\partial\Delta^2_{inf}(X_m^{out}|P_c^{out})/\partial g_x = 0$. In fact, we find $g_x = 2\left[e^r\sqrt{e^{2r}-1}(n_0+1)\right] / \left[e^{2r} + (e^{2r}-1)(2n_0+1)\right]$. Similarly, the conditional variance $\Delta^2_{inf}(P_m^{out}|X_c^{out}\rangle$ can be minimized by same optimal factor $g_p = g_x$.

Rearranging Eq. (20), we find that the mechanical oscillator is steerable by the optical pulse when

$$r > r_{steer} = \frac{1}{2}\ln\frac{2n_0+1}{n_0+1} \overset{n_0\to\infty}{\sim} \frac{1}{2}\ln 2. \qquad (22)$$

For this case, the requirement on the minimum strength of effective optomechanical interaction (for a steering of the mechanical oscillator by the optical pulse) approaches a constant, $r_{steer} = \frac{1}{2}\ln 2 = 0.35$, as the initial occupation n_0 of the oscillator increases, i.e. as $n_0 \to \infty$. Figure 4a plots the values of $E_{steer}(M|C)$ given by Eq. (20) versus r, for various values of occupation n_0.

The steering of the pulse by the mechanical oscillator can be certified if

$$E_{steer}(C|M) = 4\Delta_{inf}(X_c^{out}|P_m^{out})\Delta_{inf}(P_c^{out}|X_m^{out}) < 1. \qquad (23)$$

We find that the optical pulse is steerable by the mechanical oscillator for any n_0 and $r > 0$. Figure 4b presents the results for different n_0. For a squeezing parameter

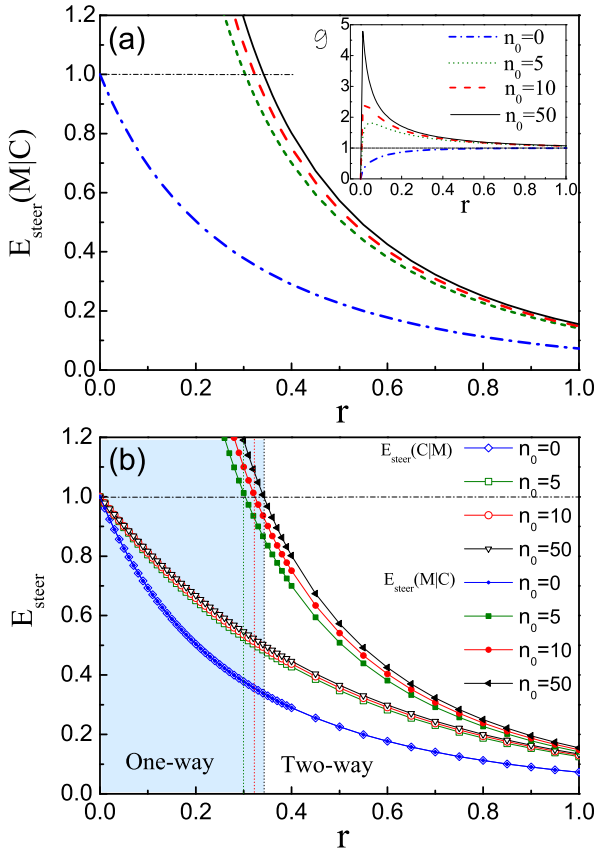

Figure 4: (Color online) Detecting steering between the oscillator and the pulse. (a) The steering nonlocality parameter $E_{steer}(M|C)$ (Eq. (20)) of the oscillator M by the cavity C, is plotted versus r for various values of the initial oscillator occupation n_0. Steering is detected when $E_{steer}(M|C) < 1$. Strong steering implies $E_{steer} \to 0$. The inset shows the optimal $g = g_x = g_p$ to minimize $E_{steer}(M|C)$. (b) Certification of one-way and two-way steering versus the squeezing parameter r. The conditional variance products according to criteria (20) and (23) are shown for various n_0.

$r \leq \frac{1}{2}\ln 2$, one-way steering is predicted, whereas for $r > \frac{1}{2}\ln 2$, two-way steering becomes possible, meaning that both mirror and pulse can steer the other remote subsystem. Clearly, the asymmetry of the steering is due to the asymmetry of the thermal effects on the two systems. As might be expected, the presence of the thermal mechanical excitation n_0 makes the steering of the oscillator, by the pulse, a more difficult challenge experimentally. This result is however of greater fundamental significance, in view of the original issues raised by Schrodinger [13], since in this case, it is the massive mesoscopic system that is being "steered", by the distant observer (the pulse system).

We find a similar prediction is given for parametric amplification in the presence of asymmetric thermal noise, as modeled by the interaction Hamiltonian $H_I = i\hbar\kappa(a^\dagger b^\dagger - ab)$, for two modes with boson operators a and b. Generally, the presence of additional thermal noise in mode b creates the possibility of one-way steering, making steering of b by a more difficult than steering of a by b. This contrasts with the result for dissipation. When mode b has additional losses, steering of a by b is more difficult than b by a [3, 24, 31].

An application of EPR-type entanglement is to enable teleportation of a quantum state [64, 65]. HWAH present a teleportation protocol based on the realisation of continuous variable teleportation using optical fields. The teleportation fidelity is given by the overlap of the reconstructed state ρ_{out} and an arbitrary quantum state $|\psi_{in}\rangle$: $F = \langle\psi_{in}|\rho_{out}|\psi_{in}\rangle$ [65]. For coherent input states, and where systems are symmetric, the fidelity is given by the entanglement parameter of Duan et al. [55], $F = 1/(1+\Delta_{ent})$. The value of $F > 1/2$ ($\Delta_{ent} < 1$) is required to do better than an optimal classical strategy [66]. However, to teleport with security, so that the quality of the state transported is sufficiently high that there can be no replica states of the same or better quality at another location, higher fidelities are necessary [23], $F > 2/3$. This requires $\Delta_{ent} < 1/2$ in the CV case, the level of correlation (6) given by symmetric steering.

D. Mechanical decoherence

The work of Ref. [46] also studies the predictions for Δ_{ent} in the presence of mechanical decoherence. Their work presents predictions showing $\Delta_{ent} < 0.5$, which is sufficient to demonstrate the steering (by (6)), for large thermal bath excitation numbers $\bar{n}$, provided the mechanical quality factor $Q_m = \omega_m/\gamma$ is high, of order $\sim 10^5$, and provided the oscillator is precooled to the ground state ($n_0 \sim 0$). In this case, the detection of the steering is clearly more challenging, though in principle feasible.

The results from the previous section however indicate a more promising prediction if the asymmetric entanglement and steering criteria are used. Here, the sensitivity of the entanglement to the initial occupation n_0 of the oscillator is greatly reduced, and detection of entanglement and steering becomes possible at higher n_0, for lower, more accessible values of squeeze parameter r. This result changes the implication for the effect of mechanical decoherence by broadening the available parameter range available for detection of EPR-type entanglement.

To give an indication of this, we have analysed the detailed model presented by HWAH, for the feasibility of detecting entanglement and steering using the asymmetric criteria. Details are given in Appendix B. The model focuses on the regime of parameters for which $g \ll \kappa \ll \omega_m$, which would justify the idealised approach given by them that is described in the previous Section. HWAH define dimensionless parameters $\eta = \kappa/\omega_m$, $\xi = g/\kappa$, and $\epsilon = \gamma\tau$ where γ is the decoherence decay rate, and use their model to arrive at optimal choices of these parameters, for the detection of Δ_{ent} in the presence of the mechanical heat bath with occupation number

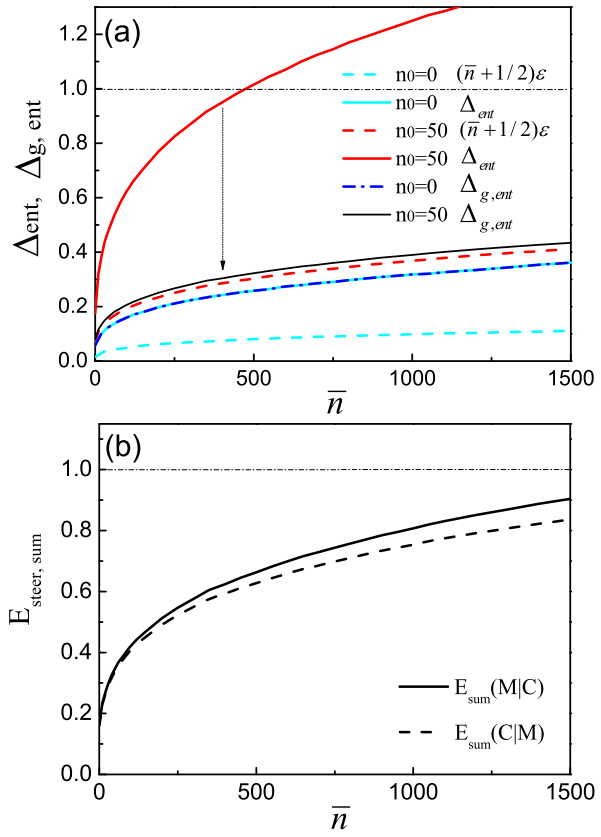

Figure 5: (Color online) Entanglement and steering in the presence of mechanical decoherence. (a) The entanglement Δ_{ent} and $\Delta_{g,ent}$ (Eq. 24) including the effect of mechanical decoherence. Here $\bar{n}$ is the thermal occupation of the associated bath. The $\Delta_{g,ent}$ is plotted with the optimal gain factor ($g = g_x = g_p$), whereas Δ_{ent} corresponds to the choice $g = 1$. The $\Delta_{g,ent}$ predicts a lower variance for $n_0 = 50$ (black solid) in comparison with Δ_{ent} (red solid). For $n_0 = 0$, the optimal value is $g = 1$, and the results for Δ_{ent} and $\Delta_{g,ent}$ agree (blue dash-dotted) and (light blue solid). The values of $(\bar{n} + \frac{1}{2})\varepsilon$ are plotted as the light blue dashed line ($n_0 = 0$) and the red dashed line ($n_0 = 50$). (b) Detection of two-way steering in the presence of mechanical decoherence for the case $n_0 = 50$. Here we plot $E_{steer,sum}$ and use the sum steering criteria of Eqs. (B5) and (B10).

$\bar{n}$, for an initial excitation n_0. The value of $\bar{n}$ depends on the temperature of the bath.

HWAH present results using the symmetric sum criterion Δ_{ent}. To enable a more direct comparison, we also consider the sum criteria, but generalised to allow for asymmetry i.e. we consider the asymmetric entanglement and steering in the sum format, given by criteria (15) and (3). The entanglement witness (15) is normalised, and is written

$$\Delta_{g,ent} = \Delta_{g,ent}|_{\gamma=0} + (2\overline{n}+1)\epsilon/\left(1+g_x g_p\right), \tag{24}$$

where $\Delta_{g,ent}|_{\gamma=0}$ is the value with no decoherence. The asymmetric entanglement condition $\Delta_{g,ent}$ becomes Δ_{ent} with the choice $g = g_x = g_p = 1$, and this prediction for the parameters chosen by HWAH is replicated in Fig. 5a, for the two values of n_0. By optimizing g, the $\Delta_{g,ent}$ can be reduced, to allow better predictions for entanglement.

The values $\Delta_{ent}|_{\gamma=0} = \Delta_{g,ent}|_{\gamma=0}$ where $g = g_x = g_p = 1$ reported by HWAH correspond to those with no mechanical decoherence, and in the analysis of HWAH are obtained from the full Langevin model. However, assuming the parameter range is consistent with $g \ll \kappa \ll \omega_m$, the solutions $\Delta_{ent}|_{\gamma=0}$ and $\Delta_{g,ent}|_{\gamma=0}$ cannot deviate significantly from those obtained in the idealised model given by the solutions (12). Hence, we obtain an approximate prediction for the asymmetric criteria by using the idealised model to solve for r, given the values for Δ_{ent} (for the given n_0). This enables the reconstruction of the asymmetric prediction for $\Delta_{g,ent}|_{\gamma=0}$, which for the higher value of $n_0 = 50$, is considerably lower than $\Delta_{ent}|_{\gamma=0}$. We then give a possible prediction for the entanglement for values considered reasonable by HAWH, by selecting the choice $\epsilon = \epsilon_{opt}$ given in their Fig. 2 (Appendix B).

The resulting predictions for entanglement detected by the symmetric and asymmetric witnesses is plotted in Fig. 5a, and shows the enhanced possibility to detect entanglement in the presence of thermal mechanical decoherence, without the need to use laser cooling to reduce the value of n_0, if one uses the asymmetric criteria. The analysis for steering is also given in the Appendix B. The observation of $\Delta_{ent} < 0.5$ is sufficient to verify steering, and this prediction can be read directly from the results already presented in Ref. [46]. However, we present the actual prediction for the steering parameter, optimised for g in Fig. 5b. As for entanglement, the results indicate the potential to detect two-way steering in the presence of thermal mechanical decoherence, without the need to use laser cooling to reduce the value of n_0.

E. Measurement of EPR steering

Our calculations suggest that steering between a mechanical oscillator and a pulse is distinctly feasible. The method of detecting steering must be considered carefully, to ensure a demonstration of quantum nonlocality [35] .

To verify the steering, one needs to measure the quadrature phase amplitudes $X_A^{out} \equiv X_c^{out}$ and $P_A^{out} \equiv P_c^{out}$ of the blue-detuned output pulse, at A, and also (in principle simultaneously) at a different location, those of the final state of the mechanical oscillator, at B. The proposed scheme of HWAH enables such measurements to be made. The output pulse measurements are made with a homodyne detector, as depicted in Fig. 1. A proposal for measuring the final quadratures of the mechanical oscillator is outlined in HWAH. A second red-detuned pulse is coupled to the oscillator, so that the output pulse and final mechanical quadratures, X_B^{out}, P_B^{out} and X_m^{out}, P_m^{out}

respectively, are given by [46]

$$\begin{aligned} X_B^{out} &= -e^{-r'}X_B^{in} - \sqrt{1-e^{-2r'}}P_m^{in}, \\ P_B^{out} &= -e^{-r'}P_B^{in} + \sqrt{1-e^{-2r'}}X_m^{in}, \\ X_m^{out} &= e^{-r'}X_m^{in} + \sqrt{1-e^{-2r'}}P_B^{in}, \\ P_m^{out} &= e^{-r'}X_m^{in} - \sqrt{1-e^{-2r'}}X_B^{in}, \end{aligned} \tag{25}$$

where r' is the interaction strength for the second pulse. In the limit of large $r' \to \infty$, the output pulse quadratures are a measure of the original quadratures of the mechanical oscillator: $X_B^{out} = -P_m^{in}$ and $P_B^{out} = X_m^{in}$. With this assumption, measurement of the quadratures X_A^{out}, P_A^{out} and X_B^{out}, P_B^{out} of the two output pulses A and B will enable demonstration of the steering nonlocality, in accordance with criterion (2). The quadrature measurements are performed via homodyne detection, as illustrated in Fig. 1b.

Since the distributions are predicted to be Gaussian, by the theory of Refs. [46, 47, 60], the procedure used in the experiment [2] involving a variable control g would enable measurement of the variances of the conditional distributions, with only a minor adjustment of the procedure for measuring $\Delta_{ent} = \frac{1}{2}\Delta_{epr}$. The method outlined in Ref. [46] using optical homodyne tomography would enable verification of the Gaussian prediction, and evaluation of the conditional distributions, for a rigorous demonstration of the EPR steering nonlocality.

For rigorous EPR tests, the measurement time T_D of the mechanical oscillator quadrature amplitudes also needs to be considered. This time is limited by the second pulse duration and cavity interaction time, which ideally would be short enough to enable a spacelike interval between the measurement events at A and B. On the other hand, the time must be long enough that the interaction strength r' enables an accurate measurement of the mechanical quadratures. The use of squeezed pulses would enhance the sensitivity of the measurements, by reducing the noise in X_B^{in} (P_B^{in}), for the measurements of X^{out} and P^{out} respectively.

F. Entanglement and steering between two mechanical oscillators

It would be a challenge to demonstrate steering between two massive systems. Bipartite steering entanglement between two mechanical oscillators can be achieved, in principle, by swapping the entanglement between the oscillator $m1$ at location A and the output pulse at location B, to an entanglement between the oscillator $m1$ at A and a second mechanical oscillator $m2$ at location B (Fig. 6). Thus, we note from the input/ output relations that one can EPR entangle two oscillators, if the first entangling pulse subsequently interacts with a second cavity. Using relation Eq. (12)

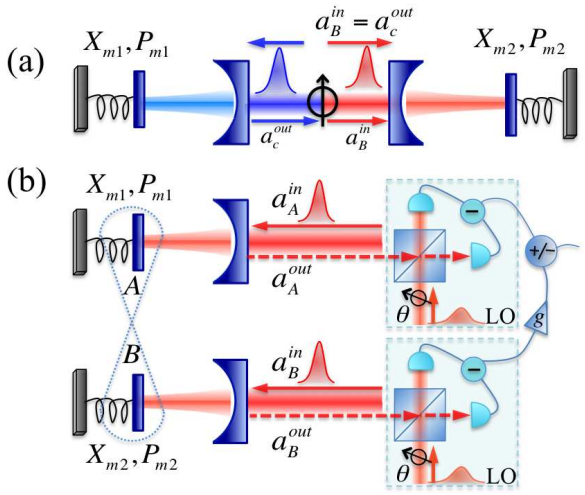

Figure 6: (Color online) Entangling two oscillators: (a) Generation of the entanglement takes place when the output of the first cavity is injected into the second cavity, as red-detuned. The final states of the two oscillators at A and B will be entangled. (b) The entanglement can be verified, at a later stage, using two red detuned pulses, and the homodyne scheme set up as depicted, to measure the conditional inference variances $\Delta_{inf}X_{mj}$ and $\Delta_{inf}P_{mj}$.

$$\begin{aligned} X_c^{out} &= -e^{r}X_c^{in} - \sqrt{e^{2r}-1}P_{m1}^{in}, \\ P_c^{out} &= -e^{r}P_c^{in} - \sqrt{e^{2r}-1}X_{m1}^{in}, \\ X_{m1}^{out} &= e^{r}X_{m1}^{in} + \sqrt{e^{2r}-1}P_c^{in}, \\ P_{m1}^{out} &= e^{r}P_{m1}^{in} + \sqrt{e^{2r}-1}X_c^{in}, \end{aligned} \tag{26}$$

as above, we see the first blue-detuned output pulse is entangled with the final quadratures of the mechanical oscillator (1). In the limit of large squeezing parameter r, the relations are $X_{m1}^{out} = -P_c^{out}$ and $P_{m1}^{out} = -X_c^{out}$. The output (of the first) pulse is then red-detuned relative to and incident on a second mechanical oscillator system ($m2$), so that the input-output relations (25) hold

$$\begin{aligned} X_B^{out} &= -e^{-r'}X_B^{in} - \sqrt{1-e^{-2r'}}P_{m2}^{in}, \\ P_B^{out} &= -e^{-r'}P_B^{in} + \sqrt{1-e^{-2r'}}X_{m2}^{in} \\ X_{m2}^{out} &= e^{-r'}X_{m2}^{in} + \sqrt{1-e^{-2r'}}P_B^{in}, \\ P_{m2}^{out} &= e^{-r'}X_{m2}^{in} - \sqrt{1-e^{-2r'}}X_B^{in}. \end{aligned} \tag{27}$$

In the limit of large r', we find $X_{m2}^{out} = P_B^{in}$ and $P_{m2}^{out} = -X_B^{in}$ so that the entanglement has been swapped into that of the mechanical oscillator. The relations between the quadratures of the mechanical oscillators is $X_{m2}^{out} = -X_{m1}^{out}$ and $P_{m2}^{out} = P_{m1}^{out}$ as $a_B^{in} = a_c^{out}$. We note that similar bipartite entanglement could potentially be realised by schemes that use two-mode entangled light fields [67].

IV. EPR STEERING BETWEEN ATOMIC ENSEMBLES

We next examine the possibility for steering between two macroscopic room temperature atomic ensembles. For this system, an EPR-type entanglement has already been realised using the criterion (4). In this case, there is symmetry between the two ensembles, and the asymmetric criteria for entanglement prove not to be so useful. However, to enhance detection of steering, it becomes essential to measure the conditional EPR paradox (steering) criterion Eq. (2), and to devise a measurement scheme which enables separate local measurement on each system.

A. Generation of EPR entanglement

The experiments of Julsgaard, Krauter, Muschik and co-workers [49–51] achieve entanglement of two macroscopic spatially separated atomic ensembles. A schematic diagram of their experiments is given in Fig. 7a. Entanglement is detected by measurement of $\Delta_{ent} < 1$, using the criteria of Eqs. (4) and (13) [55]. The experiment does not yet achieve steering, for two reasons. First, it has not been shown that an EPR paradox or steering correlation criterion of the type discussed in Refs. [39, 48] has been satisfied. The noise reduction of $\Delta_{ent} < 0.5$ (Eq. (6)) would be sufficient to demonstrate this, as would conditional variance measurements that satisfy Eq. (2). Second, the EPR observables, which in this case are the collective atomic operators, are not each measured locally.

Analysis of the theoretical models given in Refs. [49, 51, 68] suggest that a demonstration of steering is within experimental reach. We summarise the theory and the associated experiments. The two spatially separated atomic ensembles are denoted by A and B, and Schwinger collective spins, $J^X_{A/B}$, $J^Y_{A/B}$, $J^Z_{A/B}$ are defined for each atomic ensemble, which each contain N atoms. The operators are defined with respect to two atomic levels, denoted, for the jth atom in ensemble A, as $|1\rangle_j$ and $|2\rangle_j$. Thus we define: $J^Z_A = \sum_{j=1}^{N}(|1\rangle\langle 1|_j - |2\rangle\langle 2|_j)/2$; $J^X_A = \sum_{j=1}^{N}(|1\rangle\langle 2|_j + |2\rangle\langle 1|_j)/2$, and $J^Y_A = \sum_{j=1}^{N}(|1\rangle\langle 2|_j - |2\rangle\langle 1|_j)/2i$. Similar operators are defined for two selected levels of the ensemble B. Each atomic ensemble is prepared, using a detuned pump laser pulse, in an atomic spin coherent state with a large mean spin J^X, so that $\langle J^X\rangle \sim N$, and this implies the atoms are prepared in a superposition of states $|1\rangle$ and $|2\rangle$. The mean spins are equal and opposite for the ensembles A and B, i.e. $\langle J^X_A\rangle = -\langle J^X_B\rangle$. Based on the Heisenberg uncertainty relation, the steering criterion of the type (2) becomes [3]

$$\Delta_{inf} J^Z_B \Delta_{inf} J^Y_B < \frac{1}{2}|\langle J^X_B\rangle|. \tag{28}$$

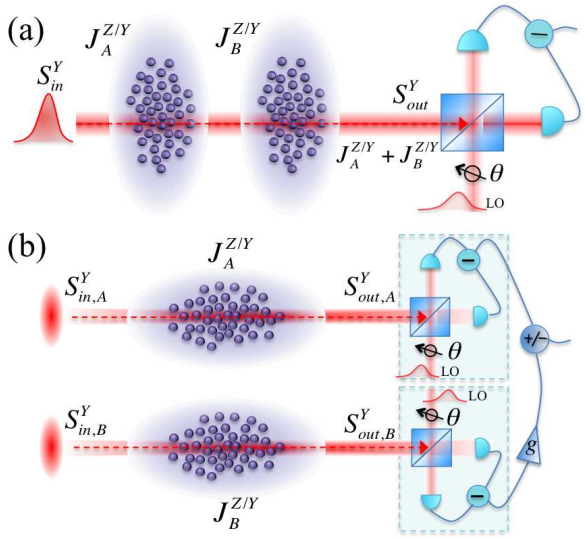

Figure 7: Schematic diagram to test the EPR steering nonlocality between atomic ensembles. (a) Depiction of the arrangement of the experiments of Refs. [49–51], which measure the sum collective spins $J^Z_A + J^Z_B$ or $J^Y_A + J^Y_B$. (b) Depiction of an experiment to demonstrate the steering between two atomic ensembles. Independent local measurements are made on the atomic ensembles A and B, by measurement of the Stokes observable S^Y of the transmitted verifying pulses. The choice of whether to measure J^Z or J^Y at each ensemble (which is made by a rotation of the atomic spin of the ensemble) is made independently and after preparation of the EPR state (which is done by the entangling pulses). The measurement process becomes more sensitive if squeezed input pulses are used, as described in the text.

The two atomic ensembles are entangled using a detuned polarised laser pulse. The laser field is described by the Stokes operators S^X, S^Y, S^Z, where S^X is the difference between photon numbers in the orthogonal X and Y linear polarisation directions; S^Y is the difference in number for polarisation modes rotated by $\pm\pi/4$; and S^Z is the difference between the photon numbers in the two circular polarised modes defined relative to the propagation direction Z. The Stokes operators are written in terms of $a_{1,2}$, the operators for the circular polarised modes. Thus,

$$\begin{aligned} S^Z &= \left(a_2^\dagger a_2 - a_1^\dagger a_1\right)/2, \\ S^X &= \left(a_2^\dagger a_1 + a_1 a_2^\dagger\right)/2, \\ S^Y &= \left(a_2^\dagger a_1 - a_2 a_1^\dagger\right)/2i. \end{aligned} \tag{29}$$

In the experiment, the light is polarised along the x direction, so that $\langle S^X\rangle \sim N_p$ where N_p is the number of photons in the optical pulse.

Following the theory of Duan et al. [68], the detuned entangling pulse propagates through an atomic ensemble, and the outputs are given in terms of the inputs according

to

$$\begin{aligned} S^Y_{out} &= S^Y_{in} + \alpha J^Z_{in}, \\ S^Z_{out} &= S^Z_{in}, \\ J^Y_{out} &= J^Y_{in} + \beta S^Z_{in}, \\ J^Z_{out} &= J^Z_{in}. \end{aligned} \tag{30}$$

The α and β are constants, and the subscripts *out* and *in* denote, for the field, the outputs and inputs to the ensemble, and, for the ensemble, the initial and final states. The β is reversed in sign for the second ensemble, so that after successive interaction with both ensembles, the final output is given in terms of the first input as

$$\begin{aligned} S^Y_{out} &= S^Y_{in} + \alpha(J^Z_{in,A} + J^Z_{in,B}), \\ S^Z_{out} &= S^Z_{in}, \\ J^Y_{out,A} + J^Y_{out,B} &= J^Y_{in,A} + J^Y_{in,B}, \\ J^Z_{out} &= J^Z_{in}. \end{aligned} \tag{31}$$

Here the subscripts A, B denote the spin operators for the A, B ensemble. As described in the Refs. [49, 68], provided α is large enough, the field output S^Y_{out} gives a measure of the collective spin $J^Z_A + J^Z_B$, which is a constant of the motion i.e. not affected by the interaction process. The Stokes parameter S^Y_{out} of the output field is measured, by polarising beam splitters and detectors, and the ensembles prepared in the state for which ideally the value of $J^Z_A + J^Z_B$ is known and constant. In practice, the preparation implies a state with reduced noise level in $J^Z_A + J^Z_B$. The collective spin $J^Y_A + J^Y_B$ is also a constant of the motion, and hence the ensembles can be prepared via a second pulse (and by rotating the atomic spin) in a state with reduced fluctuation in $J^Y_A + J^Y_B$. The reduced fluctuation in the noise levels according to

$$\Delta_{ent} = \frac{\Delta^2(J^Z_A + J^Z_B) + \Delta^2(J^Y_A + J^Y_B)}{\left|\langle J^X_A\rangle\right| + \left|\langle J^X_B\rangle\right|} \; < \; 1 \tag{32}$$

signifies entanglement between the two atomic ensembles [55]. Details of how the Δ_{ent} and the mean spin $\langle J^X_{A/B}\rangle$ are measured are given in the Refs. [49, 68].

The key point, from the perspective of this paper, is that the field-atom solutions Eq. (31) give no lower bound to the amount of noise reduction in $J^Z_A + J^Z_B$ and $J^Y_A + J^Y_B$ that is possible. The solutions Eq. (30) on which the prediction is based are valid in the limit where damping effects can be neglected. Duan et al. [68] have analysed full atomic solutions, and shown this regime is achievable when $N \sim N_p$ and provided the field detunings are much greater than spontaneous emission rates. Hence, generation of the EPR paradox between the two ensembles is predicted possible in principle using this technique, since enough EPR correlation will imply steering, by (6).

The experiments [49, 50] detect entanglement by measurement on a verifying pulse that is transmitted through both ensembles. Modification is needed for an EPR experiment. One possible strategy is to use two verifying pulses, defined with Stokes parameters $S^{X,Y,Z}_A$, $S^{X,Y,Z}_B$ respectively, one propagating through each ensemble A and B respectively (as shown in Fig. 7b). The outputs in terms of the inputs are given by the solutions Eq. (30), so that

$$\begin{aligned} S^Y_{out,A} &= S^Y_{in,A} + \alpha J^Z_{in,A}, \\ S^Y_{out,B} &= S^Y_{in,B} + \alpha J^Z_{in,B}. \end{aligned} \tag{33}$$

Measurement of $S^Y_{out,A}$ at one location, and $S^Y_{out,B}$ at the other location enables local determination of J^Z_A and J^Z_B, as required for a test of EPR nonlocality. The local measurements of J^Y_A and J^Y_B can be made similarly. The sensitivity of the measurement of the collective atomic spins $J^Z_{A/B}$ would be improved if the input fields are "squeezed", so that, for example, when measuring J^Z_A and J^Z_B, squeezed fields with $\Delta S^Y_{in,A} \to 0$ and $\Delta S^Y_{in,B} \to 0$, respectively, are used.

B. Detailed calculation of steering for an engineered dissipative system

The recent experiment of Krauter et al. [50] employs an engineered dissipative process to generate a long-lived entanglement between the atomic ensembles. Entanglement values of $\Delta_{ent} \sim 0.9$ have been realised experimentally. We therefore analyse in more depth the theory presented by Muschik, Polzik and Cirac (MPC) [51, 52] for the experiment, to calculate the degree of EPR steering predicted for the schematic set-up of Fig. 7b, given the parameters of their experiment.

The MPC model introduces operators $\tilde{A} = \mu J^-_A + v J^+_B$, $\tilde{B} = \mu J^-_B + v J^+_A$, where $J^{\pm}_{A/B}$ denote collective spin operators with $J^- = \frac{1}{\sqrt{N}}\sum_{j=1}^{N} |\uparrow\rangle\langle\downarrow|_j$ and $J^+ = \frac{1}{\sqrt{N}}\sum_{j=1}^{N} |\downarrow\rangle\langle\uparrow|_j$ such that $J^Y = (J^+ + J^-)/2$ and $J^Z = i(J^+ - J^-)/2$, and $\mu^2 - \nu^2 = 1$. The μ and ν characterise a squeezed state with squeeze parameter r, where $\mu = \cosh(r)$ and $\nu = \sinh(r)$. The correlations are described by a master equation $d_t\rho = d\frac{\Gamma}{2} \times (\tilde{A}\rho\tilde{A}^\dagger - \tilde{A}^\dagger\tilde{A}\rho + \tilde{B}\rho\tilde{B}^\dagger - \tilde{B}^\dagger\tilde{B}\rho + H.c.) + \mathcal{L}_{noise}\rho$, where ρ is the atomic density operator, d is the optical depth of an ensemble, Γ is the single atom radiative decay, and $\mathcal{L}_{noise}\rho$ describes undesired processes such as single atom spontaneous emission noise. The Linblad terms given in the parentheses drive the system into the EPR state [50]. Other parameters are the number of atoms $N_\uparrow$ and $N_\downarrow$ in each of the two levels; and the population $P_2(t) = (N_\uparrow - N_\downarrow)/N_2(t)$ where $N_2 = N_\uparrow + N_\downarrow$ is the number of atoms in the two-level system. In Appendix C of their paper [51], equations are derived for

the evolution of the atomic spins:

$$\begin{aligned}
d_t\langle (J^Z)^2\rangle &= -[\tilde{\Gamma}+d\Gamma P_2(t)]\langle (J^Z)^2\rangle \\
&\quad +\frac{N}{4}[\tilde{\Gamma}+d\Gamma P_2(t)^2(\mu^2+\nu^2)], \\
d_t\langle (J^Y)^2\rangle &= -[\tilde{\Gamma}+d\Gamma P_2(t)]\langle (J^Y)^2\rangle \\
&\quad +\frac{N}{4}[\tilde{\Gamma}+d\Gamma P_2(t)^2(\mu^2+\nu^2)], \\
d_t\langle J_A^Z J_B^Z\rangle &= -[\tilde{\Gamma}+d\Gamma P_2(t)]\langle J_A^Z J_B^Z\rangle \\
&\quad +\frac{N}{2}\mu\nu d\Gamma P_2(t)^2, \\
d_t\langle J_A^Y J_B^Y\rangle &= -[\tilde{\Gamma}+d\Gamma P_2(t)]\langle J_A^Y J_B^Y\rangle \\
&\quad -\frac{N}{2}\mu\nu d\Gamma P_2(t)^2, \qquad (34)
\end{aligned}$$

where $\tilde{\Gamma} = \Gamma_{cool}+\Gamma_{heat}+\Gamma_d$, $\Gamma_{cool}(\Gamma_{heat})$ is the total single-particle cooling (heating) rate and Γ_d is the total dephasing rate. This leads to the equation (C1) of their paper, describing the evolution of the variances $\Delta^2(J_A^{Y/Z} \pm J_B^{Y/Z})$.

To obtain the optimal prediction for steering in the Gaussian system, we modify the analysis to calculate the evolution of the conditional variances, $Var(J_A^Y|J_B^Y) = \Delta^2(J_A^Y \pm g_Y J_B^Y)$ and $Var(J_A^Z|J_B^Z) = \Delta^2(J_A^Z \pm g_Z J_B^Z)$. The conditional variances can be measured by the arrangement of Fig. 7b, which allow a relative weighting of the measurement of the collective spin of one ensemble, against that of the second ensemble. The equations are

$$\begin{aligned}
d_t Var(J_A^Y|J_B^Y) &= -[\tilde{\Gamma}+d\Gamma P_2(t)]Var(J_A^Y|J_B^Y) \\
&\quad +\frac{N(1+g_Y^2)}{4}[\tilde{\Gamma}+d\Gamma P_2(t)^2(\mu^2+\nu^2)] \\
&\quad \mp N g_Y \mu\nu d\Gamma P_2(t)^2, \\
d_t Var(J_A^Z|J_B^Z) &= -[\tilde{\Gamma}+d\Gamma P_2(t)]Var(J_A^Z|J_B^Z) \\
&\quad +\frac{N(1+g_Z^2)}{4}[\tilde{\Gamma}+d\Gamma P_2(t)^2(\mu^2+\nu^2)] \\
&\quad \pm N g_Z \mu\nu d\Gamma P_2(t)^2. \qquad (35)
\end{aligned}$$

The steady state solutions are given by

$$\begin{aligned}
&Var(J_A^Y|J_B^Y)_\infty = \\
&\frac{A_Y[\tilde{\Gamma}+d\Gamma P_{2,\infty}^2(\mu^2+\nu^2)] \mp N g_Y \mu\nu d\Gamma P_{2,\infty}^2}{[\tilde{\Gamma}+d\Gamma P_{2,\infty}]}, \\
&Var(J_A^Z|J_B^Z)_\infty = \\
&\frac{A_Z[\tilde{\Gamma}+d\Gamma P_{2,\infty}^2(\mu^2+\nu^2)] \pm N g_Y \mu\nu d\Gamma P_{2,\infty}^2}{[\tilde{\Gamma}+d\Gamma P_{2,\infty}]}, \qquad (36)
\end{aligned}$$

where $A_Y = N(1+g_Y^2)/4$ and $A_Z = N(1+g_Z^2)/4$, and we will choose

$$g_Y = -g_Z = \frac{\pm\mu\nu d\Gamma P_{2,\infty}^2}{[\tilde{\Gamma}+d\Gamma P_{2,\infty}^2(\mu^2+\nu^2)]/2} \qquad (37)$$

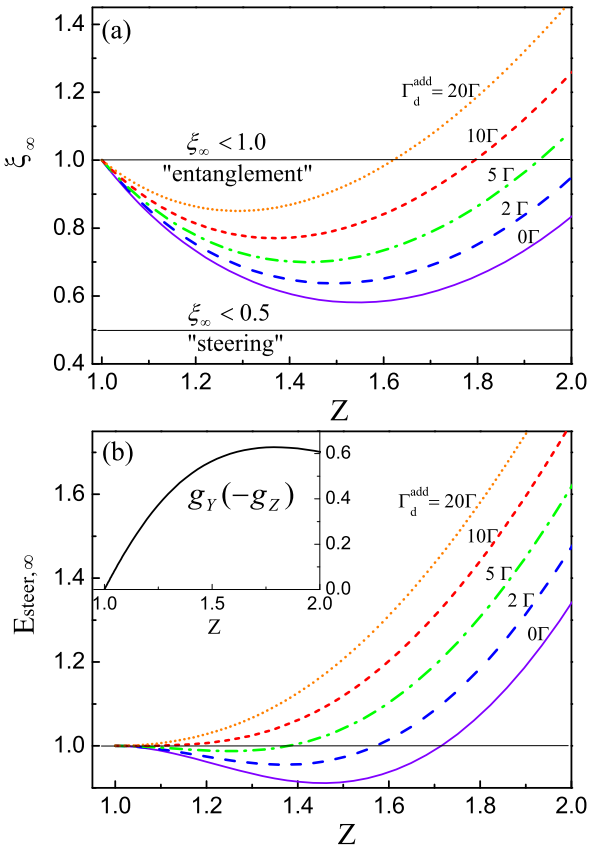

Figure 8: (Color online) Steady state EPR steering using the engineered dissipatively driven system of Muschik et al. [51]. (a) The predictions for the steady state entanglement $\Delta_{ent} = \xi_\infty$ versus $Z = (\mu - v)^{-1}$ for an optical depth $d = 30$ per ensemble. We use the parameters presented in Fig. 3 of Ref. [51]. $\xi_\infty < 1$ represents entanglement between two ensembles, and the observation of $\Delta_{ent} = \xi_\infty < 0.5$ is also sufficient to verify steering. (b) The predictions for the steering (39) using the same parameters but optimal values of gain factor g_Y and g_Z. $E_{steer,\infty} < 1$ indicates two-way steering between ensembles. The inset shows the optimal gain factor $g_Y(-g_Z)$ for minimizing $E_{steer,\infty}$. In this case $\Gamma_{cool} = \mu^2\Gamma$ and $\Gamma_{heat} = v^2\Gamma$. The dephasing rate $\Gamma_d = \Gamma_d^{rad} + \Gamma_d^{add}$ consists of a radiative part $\Gamma_d^{rad} = 2(\mu^2+v^2)\Gamma$ which is due to light-induced transitions, and an additional term Γ_d^{add} which summarizes all nonradiative sources of dephasing. The violet line is for pure radiative damping, $\Gamma_d^{add} = 0$. Γ is the single particle decay rate.

to minimize the conditional variances. The steady state solution for $\left|\langle J_{A,B}^X\rangle\right|$ is given by Muschik et al. [51], as

$$\left|\langle J_{A,B}^X\rangle\right|_\infty = \frac{N}{2}P_{2,\infty} \qquad (38)$$

for $t \to \infty$.

The steady state steering $E_{steer,\infty}$ is then given as

$$E_{steer,\infty} = \frac{\sqrt{Var(J_A^Y|J_B^Y)_\infty Var(J_A^Z|J_B^Z)_\infty}}{\frac{1}{2}\left|\langle J_A^X\rangle\right|_\infty}. \qquad (39)$$

The entanglement is

$$\Delta_{g,ent} = \xi_{\infty,g} = \frac{Var(J_A^Y|J_B^Y)_\infty + Var(J_A^Z|J_B^Z)_\infty}{\left(\left|\langle J_A^X\rangle\right|_\infty + \left|g_Y g_Z||\langle J_B^X\rangle\right|_\infty\right)/2}, \quad (40)$$

where we also use introduce the notation ξ_∞ used by MPC: ξ_∞ is the value of Δ_{ent} in the steady state. In fact, due to the symmetry of the two systems, $\Delta_{g,ent}$ is minimized by the optimal gain factor $g_Y = -g_Z = 1$, and hence agrees with Eq. (15) in Ref. [51]. The steady state entanglement $\xi_\infty = \Delta_{ent}$ is plotted in Fig. 8a.

We plot the optimal steering prediction, for the parameters chosen by Muschik et al. [51] in their Fig. 3. Of course, the observation of $\Delta_{ent} = \xi_\infty < 0.5$ (by (6)) is also sufficient to verify steering, but the noise reduction in their case is not enough to establish this. We therefore present the actual prediction for the steering, optimised for $g_Y(g_Z)$, in Fig. 8b. Steering is clearly more difficult to generate than entanglement, with values of $E_{steer,\infty} \sim 0.9$ being predicted for mainly pure radiative damping, for which values of entanglement $\Delta_{ent} \sim 0.6$ are predicted. Given that the experiment has achieved steady state entanglement, a measurement of steering would not seem an impossibility, however, even for room temperature atoms.

V. SUMMARY

In summary, the EPR paradox entanglement studied in this paper confirms an inconsistency of local realism with the completeness of quantum mechanics, and is evidence for the form of nonlocality called "EPR steering". We have analysed the possibility of realising such steering for two physical systems: pulsed cavity optomechanics, and spatially separated macroscopic atomic ensembles. We propose how steering might be generated, verified, and optimised in each case.

Especially, we note that for the first system, because thermal noise is more significant for the mechanical oscillator than for the optical mode, the use of asymmetric entanglement and steering criteria will greatly increase the possibility of observing both entanglement and steering. This is true even where there is a significant initial occupation number of the oscillator and in the presence of mechanical decoherence. We find a regime of one-way steering is possible, where the optical system can be steered by, but cannot steer, the mechanical oscillator.

For the second system, EPR steering is predicted within the parameter range of the experiment, provided nonradiative sources of atomic dephasing are not too large. It becomes essential however to modify the experimental design to ensure detection of two local EPR observables, so that conditional measurements can be realised.

In conclusion, we have considered detailed theories for entanglement generation in two sorts of massive systems. The theories model the major sources of decoherence, (dissipation and thermal reservoirs) and for the case of gas ensembles have been partially verified experimentally. Our work reveals that detection of steering is more challenging than detection of entanglement, but is predicted feasible, for accessible parameter regimes.

Acknowledgments

We thank P. D. Drummond, W. Bowen and Sebastian G. Hofer for useful discussions and information. We acknowledge support from the Australian Research Council for funding via ACQAO COE, Discovery, and DECRA grants. Q. Y. H. wishes to thank the support by the National Natural Science Foundation of China under Grant No. 11121091.

Appendix A: Proofs

We outline the derivation of the EPR entanglement criteria used in this paper. Assuming separability, and that the variance of a mixture must not be less than the average of the variances of its components, we can write [55]

$$\begin{aligned}
&\Delta^2(X_B - g_x X_A) + \Delta^2(P_B + g_p P_A) \\
\geq\ & \sum_R P_R(\Delta_R^2(X_B - g_x X_A) + \Delta_R^2(P_B + g_p P_A)) \\
=\ & \sum_R P_R[\langle X_B^2\rangle_R + g_x^2\langle X_A^2\rangle_R - 2g_x\langle X_B\rangle_R\langle X_A\rangle_R] \\
& + \sum_R P_R[\langle P_B^2\rangle_R + g_p^2\langle P_A^2\rangle_R + 2g_p\langle P_B\rangle_R\langle P_A\rangle_R] \\
& - \sum_R P_R\langle X_B - g_x X_A\rangle_R^2 - \sum_R P_R\langle P_B + g_p P_A\rangle_R^2 \\
=\ & \sum_R P_R(\Delta_R^2 X_B + \Delta_R^2 P_B + g_x^2\Delta_R^2 X_A + g_p^2\Delta_R^2 P_A).
\end{aligned} \quad (A1)$$

Here, the subscript R denotes the variance or average for the state depicted by R (namely ρ_A^R or ρ_B^R). Separability implies the factorisation, for example, $\langle X_A X_B\rangle_R = \langle X_A\rangle_R\langle X_B\rangle_R$. For any quantum state, uncertainty relations follow from $\Delta X_B \Delta P_B \geq |\langle[X_B, P_B]\rangle|/2 = 1/4$. The local uncertainty relation is $\Delta^2 X_B + \Delta^2 P_B \geq 1/2$ and $\Delta^2(g_x X_A) + \Delta^2(g_y P_A) \geq g_x g_p/2$ (we use the identity $x^2 + y^2 \geq 2xy$, for x, y real numbers). The inequality thus becomes

$$\Delta^2(X_B - g_x X_A) + \Delta^2(P_B + g_p P_A) \geq (1 + g_x g_p)/2, \quad (A2)$$

which if violated confirms entanglement between the modes denoted by A and B. For $g_x = g_p = 1$, the criterion reduces to the symmetric criterion for entanglement used by HWAH.

We now note that EPR steering criteria can be derived, from the above proof, by using the LHS model of Ref. [13]. In this case, the second site that is being steered remains with a quantum restriction, meaning that the uncertainty relation holds for it, but the steering site becomes unconstrained (except as a local hidden variable site). In that case, the right side bound is replaced by either $1/2$ or $g_x g_p/2$ depending of whether we wish to show A steer B, or B steers A respectively. For $g_x = g_p = 1$, we obtain the criterion (6) for EPR steering.

Criteria involving the product of variances can also be derived (as in Refs. [57, 58]):

$$\begin{aligned}
&\Delta^2(X_B - g_x X_A)\Delta^2(P_B + g_p P_A) \\
&\geq [\sum_R P_R \Delta_R^2 (X_B - g_x X_A)][\sum_R P_R \Delta_R^2 (P_B + g_p P_A)] \\
&= \sum_R P_R[\Delta_R^2 X_B + g_x^2 \Delta_R^2 X_A] \times \sum_R P_R[\Delta_R^2 P_B + g_p^2 \Delta_R^2 P_A] \\
&\geq \{\sum_R P_R[\Delta_R^2 X_B \Delta_R^2 P_B + g_x^2 g_p^2 \Delta_R^2 X_A \Delta_R^2 P_A \\
&\quad + g_x^2 \Delta_R^2 X_A \Delta_R^2 P_B + g_p^2 \Delta_R^2 P_A \Delta_R^2 X_B]^{1/2}\}^2 \\
&\geq \frac{1 + g_x^2 g_p^2 + 2|g_x g_p|}{16} = \left(\frac{|g_x g_p| + 1}{4}\right)^2 . \qquad \text{(A3)}
\end{aligned}$$

Here we have used the standard Cauchy Schwarz inequality and the Heisenberg uncertainty relations. Hence, entanglement is verified when

$$\Delta^2(X_B - g_x X_A)\Delta^2(P_B + g_p P_A) < \left(\frac{|g_x g_p| + 1}{4}\right)^2 . \quad \text{(A4)}$$

Appendix B: Mechanical decoherence

We analyse the model for mechanical deocherence presented by HWAH [46], for the feasibility of detecting entanglement and steering using the asymmetric criteria. The model focuses on the regime of parameters for which $g \ll \kappa \ll \omega_m$. Dimensionless parameters $\eta = \kappa/\omega_m$, $\xi = g/\kappa$ and $\epsilon = \gamma\tau$ are defined, where γ is the decoherence decay rate, and HWAH use their model to arrive at optimal choices of these parameters, for the detection of Δ_{ent} in the presence of the mechanical heat bath with occupation number $\bar{n}$, for an initial excitation n_0. The value of $\bar{n}$ depends on the temperature of the bath.

HWAH arrive at solutions (Eq. (21) of their paper) for the quadrature phase amplitudes,

$$\begin{aligned}
X_m^{out} &= X_m^{out}|_{\gamma=0} + \sqrt{\epsilon} F_s, \\
P_m^{out} &= P_m^{out}|_{\gamma=0} + \sqrt{\epsilon} F_c, \qquad \text{(B1)}
\end{aligned}$$

where the additional noise operators F_s and F_c are due to thermal mechanical noise. Thermal noise is neglected for the optical fields, for which $X_c^{out} \sim X_c^{out}|_{\gamma=0}$. Also, the effect of damping is justified to be small compared to the effect of the thermal noise term. The model leads, under the approximations that justify a perturbative expansion for the symmetric entanglement

$$\Delta_{ent} = \Delta_{ent}|_{\gamma=0} + (\bar{n} + \frac{1}{2})\epsilon. \qquad \text{(B2)}$$

We now analyse the prediction for the asymmetrical entanglement criterion. We find, using (B1), that

$$\begin{aligned}
\Delta^2(X_m^{out} + g_x P_c^{out}) &= \Delta^2(X_m^{out} + g_x P_c^{out})|_{\gamma=0} + \frac{\epsilon}{2}(\overline{n} + \frac{1}{2}), \\
\Delta^2(P_m^{out} + g_p X_c^{out}) &= \Delta^2(P_m^{out} + g_p X_c^{out})|_{\gamma=0} + \frac{\epsilon}{2}(\overline{n} + \frac{1}{2}) \qquad \text{(B3)}
\end{aligned}$$

because the extra noise arises solely from the mechanical quadratures.

For a direct comparison, we consider the entanglement and steering in the sum format, given by criteria (15) and (3). The entanglement witness (15) is normalised, and becomes (using (B3))

$$\Delta_{g,ent} = \Delta_{g,ent}|_{\gamma=0} + (2\overline{n} + 1)\epsilon / (1 + g_x g_p) . \qquad \text{(B4)}$$

The prediction for the parameters chosen by HWAH in their Fig. 2 is replicated in the plot of Fig. 5a for $g = g_x = g_p = 1$, for the two values of n_0 considered by them. By optimizing g, the $\Delta_{g,ent}$ can be reduced. The values $\Delta_{ent}|_{\gamma=0}$ reported by HWAH correspond to those with no mechanical decoherence, and in the analysis of HWAH are obtained from the full Langevin model. However, since the parameter range considered by HAWH is consistent with $g \ll \kappa \ll \omega_m$, the solutions $\Delta_{ent}|_{\gamma=0}$ and $\Delta_{g,ent}|_{\gamma=0}$ cannot deviate significantly from those obtained in the idealised model given by the solutions (12). Hence, we approximate the prediction for the asymmetric criteria by solving the values given for $\Delta_{ent} = \Delta_{EPR}/2$ (for the n_0) for r. This enables the reconstruction of the asymmetric prediction for $\Delta_{g,ent}|_{\gamma=0}$, which for the higher value of $n_0 = 50$, is considerably lower than $\Delta_{ent}|_{\gamma=0}$.

We then give a possible prediction for the entanglement for values considered reasonable by HAWH, by selecting the choice $\epsilon = \epsilon_{opt}$ given in their Fig. 2, and using the solution (B3). The result is plotted in Fig. 5a, and shows the possibility to detect entanglement in the presence of thermal mechanical decoherence, without the need to use laser cooling to reduce the value of n_0.

Steering is confirmed if we satisfy the sum criterion (3) which becomes

$$\begin{aligned}
E_{steer,sum}(M|C) &= 2\{\Delta^2(X_m^{out} + g_x P_c^{out}) \\
&\quad + \Delta^2(P_m^{out} + g_p X_c^{out})\} < 1. \qquad \text{(B5)}
\end{aligned}$$

Thus, we can write the left side variances once again in terms of the steering parameter for $\gamma = 0$, and the

thermal noise term, and normalise to obtain the measure of steering in the presence of mechanical decoherence:

$$E_{steer,sum}(M|C) = E_{g,sum}(M|C)|_{\gamma=0} + (2\overline{n}+1)\epsilon. \tag{B6}$$

The entanglement criterion is symmetric with respect to the two systems, whereas the steering one is not. Therefore, we also calculate

$$\Delta^2_{inf}(X_c^{out} + g_x P_m^{out}) = \Delta^2(X_c + g_x P_m^{out})|_{\gamma=0} + \frac{1}{2}g_x^2\epsilon(\bar{n}+\frac{1}{2}), \tag{B7}$$

$$\Delta^2_{inf}(P_c^{out} + g_p X_m^{out}) = \Delta^2(P_c + g_p X_m^{out})|_{\gamma=0} \tag{B8}$$

$$+ \frac{1}{2}g_p^2\epsilon(\bar{n}+\frac{1}{2}). \tag{B9}$$

Steering $(C|M)$ is confirmed if we satisfy the criterion (3) which becomes

$$E_{steer,sum}(C|M) = 2\{\Delta^2(X_c^{out} + g_x P_m^{out}) + \Delta^2(P_c^{out} + g_p X_m^{out})\} < 1, \tag{B10}$$

and then, in this case,

$$E_{steer,sum}(C|M) = E_{g,sum}(C|M)|_{\gamma=0} + (\bar{n}+\frac{1}{2})\epsilon(g_x^2 + g_p^2),$$

where the g_x and g_p are optimised again, to minimise the variances and the measure of $E_{steer,sum}(C|M)$.

We plot the optimal steering prediction in Fig. 5, for the parameters chosen by HWAH in their Fig. 2. Of course, the observation of $\Delta_{ent} < 0.5$ is sufficient to verify steering, and this prediction can be read directly from the Fig. 2 plots presented by HWAH. However, $\Delta_{ent} < 0.5$ will show steering only for $g_x = g_p = 1$, and we present the actual prediction for the steering parameter, optimised for g in Fig. 5b. As for entanglement, the results indicate the potential to detect steering in the presence of thermal mechanical decoherence, without the need to use laser cooling to reduce the value of n_0.

[1] A. Einstein, B. Podolsky, and N. Rosen, Phys. Rev. **47**, 777 (1935).
[2] Z. Y. Ou, S. F. Pereira, H. J. Kimble, and K. C. Peng, Phys. Rev. Lett. **68**, 3663 (1992).
[3] M. D. Reid *et al.*, Rev. Mod. Phys. **81**, 1727 (2009) and experiments referenced therein.
[4] Y. Wang *et al.*, Opt. Express **18**(6), 6149 (2010).
[5] B. Hage, A. Samblowski, and R. Schnabel, Phys. Rev. A **81**, 062301 (2010); T. Eberle *et al.*, Phys. Rev. A **83**, 052329 (2011); A. Samblowski *et al.*, arXiv:1011.5766v2; S. Steinlechner *et al.*, arXiv:1112.0461v2.
[6] V. Boyer, A. M. Marino, R. C. Pooser, and P. D. Lett, Science **321**, 544 (2008).
[7] K. Wagner et al., Science **321**, 541 (2008).
[8] A. Aspect, P. Grangier, and G. Roger, Phys. Rev. Lett. **49**, 91 (1982).
[9] J. F. Clauser *et al.*, Phys. Rev. Lett. **23**, 880 (1969); A. Aspect, J. Dalibard, and G. Roger, *ibid.* **49**, 1804 (1982); P. G. Kwiat *et al.*, Phys. Rev. Lett. **75**, 4337 (1995); G. Weihs *et al.*, *ibid.* **81**, 5039 (1998); W. Tittel *et al.*, *ibid.* **84**, 4737 (2000).
[10] J. C. Howell, R. S. Bennink, S. J. Bentley, and R. W. Boyd, Phys. Rev. Lett. **92**, 210403 (2004).
[11] W. P. Bowen, N. Treps, R. Schnabel, and P. K. Lam, Phys. Rev. Lett. **89**, 253601 (2002).
[12] Ch. Silberhorn *et al.*, Phys. Rev. Lett. **86**, 4267 (2001); Y. Zhang *et al.*, Phys. Rev. A **62**, 023813 (2000).
[13] H. M. Wiseman, S. J. Jones, and A. C. Doherty, Phys. Rev. Lett. **98**, 140402 (2007).
[14] S. J. Jones, H. M. Wiseman, and A. C. Doherty, Phys. Rev. A **76**, 052116 (2007).
[15] E. Schrödinger, Proc. Cambridge Philos. Soc. **31**, 553 (1935); *ibid.* **32**, 446 (1936).
[16] E. G. Cavalcanti, S. J. Jones, H. M. Wiseman, and M. D. Reid, Phys. Rev. A **80**, 032112 (2009).
[17] D. J. Saunders, S. J. Jones, H. M. Wiseman, and G. J. Pryde, Nat. Phys. **6**, 845 (2010).
[18] T. C. Ralph, Phys. Rev. A **61**, 010303(R) (1999); T. C. Ralph, Phys. Rev. A **62**, 062306 (2000);
[19] M. D. Reid, Phys. Rev. A **62**, 062308 (2000).
[20] F. Grosshans and P. Grangier, Phys. Rev. Lett. **88**, 057902 (2002).
[21] V. Scarani, H. B. Pasquinucci, N. J. Cerf, M. Dušek, N. Lütkenhaus, and M. Peev, Rev. Mod. Phys. **81**, 1301 (2009)).
[22] C. Branciard, E. G. Cavalcanti, S. P. Walborn, V. Scarani, and H. M. Wiseman, Phys. Rev. A **85**, 010301(R) (2012).
[23] F. Grosshans and P. Grangier, Phys. Rev. A **64**, 010301 (2001).
[24] S. L. W. Midgley, A. J. Ferris, and M. K. Olsen, Phys. Rev. A **81**, 022101 (2010).
[25] E. G. Cavalcanti, Q. Y. He, M. D. Reid, and H. M. Wiseman, Phys. Rev. A **84**, 032115 (2011).
[26] J. Oppenheim and S. Wehner, Science **19**, 1072 (2010).
[27] J. D. Bancal, N. Brunner, N. Gisin, and Y. C. Liang, Phys. Rev. Lett. **106**, 020405 (2011).
[28] S. J. Jones and H. M. Wiseman, Phys. Rev. A **84**, 012110 (2011).
[29] Q. Y. He, P. D. Drummond, and M. D. Reid, Phys. Rev. A **83**, 032120 (2011).
[30] N. Takei *et al.*, Phys. Rev. A **74**, 060101(R) (2006).
[31] V. Händchen *et al.*, Nature Photonics **6**, 598 (2012); K. Wagner et al., arXiv:1203.1980 [quant-ph].
[32] S. P. Walborn, A. Salles, R. M. Gomes, F. Toscano, and P. H. Souto Ribeiro, Phys. Rev. Lett. **106**, 130402 (2011).

[33] D. H. Smith *et al.*, Nature Commu. **3**, 625 (2012).
[34] A. J. Bennet *et al.*, Phys. Rev. X **2**, 031003 (2012).
[35] B. Wittmann *et al.*, New J. Phys. **14**, 053030 (2012).
[36] M. A. Rowe *et al.*, Nature **409** 791 (2001).
[37] M. Ansmann *et al.*, Nature **461**, 504 (2009).
[38] T. Opatrny and G. Kurizki, Phys. Rev. Lett. **86**, 3180 (2001); A. O. Barut and P. Meystre, Phys. Rev. Lett. **53**, 1021 (1984); K. V. Kheruntsyan, M. K. Olsen, and P. D. Drummond, Phys. Rev. Lett. **95**, 150405 (2005).
[39] A. J. Ferris, M. K. Olsen, E. G. Cavalcanti, and M. J. Davis, Phys. Rev. A **78**, 060104(R) (2008).
[40] N. Bar-Gill, C. Gross, I. Mazets, M. Oberthaler, and G. Kurizki, Phys. Rev. Lett. **106**, 120404 (2011).
[41] Q. Y. He, P. D. Drummond, M. K. Olsen, and M. D. Reid, Phys. Rev. A **86**, 023626 (2012).
[42] B. Opanchuk, Q. Y. He, M. D. Reid, and P. D. Drummond, Phys. Rev. A **86**, 023625 (2012).
[43] R. Bücker *et al.*, Nature Phys. **7**, 608 (2011).
[44] R. Bücker *et al.*, Phys. Rev. A **86**, 013638 (2012).
[45] C. Gross *et al.*, Nature **480**, 219 (2011).
[46] S. G. Hofer, W. Wieczorek, M. Aspelmeyer, and K. Hammerer, Phys. Rev. A **84**, 052327 (2011).
[47] V. Giovannetti, S. Mancini, and P. Tombesi, Europhys. Lett. **54**, 559 (2001).
[48] M. D. Reid, Phys. Rev. A **40**, 913 (1989).
[49] B. Julsgaard, A. Kozhekin, and E. S. Polzik, Nature **413**, 400 (2001).
[50] H. Krauter *et al.*, Phys. Rev. Lett. **107**, 080503 (2011).
[51] C. A. Muschik, E. S. Polzik, and J. I. Cirac, Phys. Rev. A **83**, 052312 (2011).
[52] C. A. Muschik *et al.*, J. Phys. B: At. Mol. Opt. Phys. **45** 124021 (2012).
[53] J. S. Bell, Physics **1,** 195 (1964); J. S. Bell, *Speakable and Unspeakable in Quantum Mechanics* (Cambridge University Press 1987).
[54] E. G. Cavalcanti and M. D. Reid, Journ. Mod. Opt. **54**, 2373 (2007); E. G. Cavalcanti, P. D. Drummond, H. A. Bachor, and M. D. Reid, Optics Express **17**, 18693 (2009).
[55] L. M. Duan, G. Giedke, J. I. Cirac, and P. Zoller, Phys. Rev. Lett. **84**, 2722 (2000); R. Simon, Phys. Rev. Lett. **84**, 2726 (2000).
[56] G. Giedke and J. I. Cirac, Phys. Rev. A **66**, 032316 (2002); R. Simon, E. C. G. Sudarshan, and N. Mukunda, Phys. Rev. A **36**, 3868 (1987); M. B. Plenio, Phys. Rev. Lett. **95**, 090503 (2005).
[57] V. Giovannetti, S. Mancini, D. Vitali, and P. Tombesi, Phys. Rev. A **67**, 022320 (2003).
[58] S. Mancini *et al.*, Phys. Rev. Lett. **88**, 120401 (2002).
[59] M. R. Vanner *et al.*, Proc. Nat. Ac. Sc. **108**, 16182 (2011).
[60] S. Mancini and P. Tombesi, Phys. Rev. A **49**, 4055 (1994).
[61] C. M. Caves and B. L. Schumaker, Phys. Rev. A **31**, 3068 (1985).
[62] M. D. Reid and D. F. Walls, Phys Rev A **33**, 4465 (1986).
[63] C. W. Gardiner and M. J. Collett, Phys. Rev. A **31**, 3761 (1985).
[64] C. H. Bennett *et al.*, Phys. Rev. Lett. **70**, 1895 (1993); D. Bouwmeester *et al.*, Nature **390,** 575 (1997); N. Lee *et al.*, Science **332**, 330 (2011).
[65] A. Furusawa, J. L. Sørensen, S. L. Braunstein, C. A. Fuchs, H. J. Kimble, and E. S. Polzik, Science **282**, 706 (1998); S. L. Braunstein and H. J. Kimble, Phys. Rev. Lett. **80**, 869 (1998); P. van Loock and S. L. Braunstein, Phys. Rev. A **61**, 010302(R) (1999).
[66] S. L. Braunstein, C. A. Fuchs, H. J. Kimble, and P. van Loock, Phys. Rev. A **64**, 022321 (2001); K. Hammerer, M. M. Wolf, E. S. Polzik, and J. I. Cirac, Phys. Rev. Lett. **94**, 150503 (2005).
[67] L. Mazzola and M. Paternostro, Scientific Reports **1**, 199 (2011).
[68] L. M. Duan, J. Cirac, P. Zoller, and E. Polzik, Phys. Rev. Lett. **85**, 5643 (2000).